Chaotic behavior in super regenerative detectors

Chaotic Behavior in Super Regenerative Detectors

Domine M. W. Leenaerts, *Member, IEEE*

Abstract— **In this paper the super regenerative detector, as proposed by Armstrong in 1922, will be investigated. We will show that in a simplified model the current in the circuit behaves chaotically during a small period in time after which the circuit becomes an oscillator. Armstrong was not aware of the circuits' chaotic behavior, but reported strange irregular start-ups of the oscillator. Chaotic behavior of the circuit will be demonstrated in this paper using computer simulation. During the period in which the irregularities appear, the amplification of the circuit is maximal.**

I. Introduction

In 1922, Armstrong invented the (super)regenerative circuit as a detector with higher sensitivity and selectivity as compared to other types of receivers [1]. This type of detection was often used in radio engineering in the early days following this invention. Nowadays, regenerative detectors are still used as predetection systems when very high frequencies (e.g., microwave communication) are involved [2]. The regenerative detector is favorably used in applications where simplicity and compactness outweigh the need for low noise reception. Because a single tube may be used in the receiver as well as in the transmitter, this kind of circuits is typically found in radar beacon applications.

In a super regenerative detector the inductive coupling between the plate and grid circuits of the detector tube via coil L is such that self-sustained oscillations can be built up (Fig. 1). A weak incoming signal on the same L is sufficient to start the oscillation and to amplify the incoming signal. However, amplification is only possible during the start-up time of the oscillator. Once the system oscillates or "generates," it will operate independent from the input signals and this is not desired for a detector. To prevent this situation, the oscillation is periodically quenched, with a frequency much lower than the free oscillation frequency. Energy is supplied to the system to control the oscillation. The process of supplying energy to reinforce the oscillations is called regeneration. Now, each time during the start-up of the oscillation, the system can detect an incoming signal. Then this signal initiates the oscillation, which will subsequently be quenched by the supplied energy. Regeneration of the oscillation will start at the detection of a new signal. Normally the quench voltage is applied to the plate of the tube (see Fig. 1) and inductively fed back to the oscillators' grid circuit.

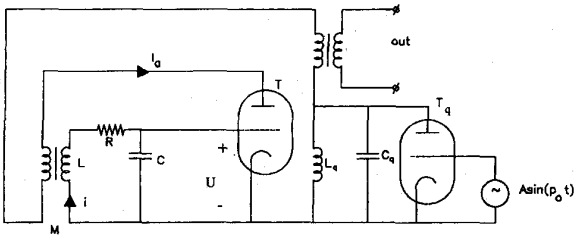

Fig. 1. The super regenerative detector. In his paper Armstrong did use Western Electric Type L tubes but did not give information on the other components. The sources biasing the tubes are left out for convenience.

Although the basic operation of the circuit was understood, there still was the problem of the characteristic noise generated in those circuits. One assumed that the characteristic noise, which could be heard in the earphones, was caused by the noise from the circuits components (e.g., tubes) and amplified during the start-up of the oscillation. In this paper we will show that the behavior of a simplified model of the detector is chaotic. This behavior exhibits during the start-up of the free oscillations under certain conditions. Before operating as an oscillator, there is a period in which the behavior of the current is irregular. It turns out that the detector also has the maximal amplification factor when it operates chaotically.

It is interesting to notice that up to now the forced van der Pol oscillator, as published in 1927, was believed to be the earliest known circuit to have chaotic solutions [3], [4]. The circuit of Armstrong now seems to be the oldest one with noticed irregular behavior. Both Armstrong and Van der Pol did not realize that their circuits produced chaos. In the past, many forced oscillators have been investigated [5]–[7]. The behavior of these circuits was chaotic during the complete operating mode. In contrast, the circuit of Armstrong shows a chaotic behavior only during a small interval of time. The chaotic behavior is therefore finite in time.

The paper is organized as follows. In Section II, we will discuss the working of the regenerative detector as developed by Armstrong and in Section III we will introduce a simplified model that will be used for the computer simulations. In Section IV it will be shown that the oscillations start up chaotically, while Section V deals with the amplification and sensitivity of the detector. Conclusions are given in Section VI.

II. The Regenerative Detector

Let us start with the simple tuned grid oscillator, depicted in Fig. 2. This oscillator is built up around the triode tube T. The circuit consisting of the LRC-network is normally called

Manuscript received October 20, 1994; revised March 20, 1995 and June 29, 1995. This work was supported in part by the Dutch Foundation for Research (STW) under Project EEL44.3386. Part of this work was conducted at the Department of Electrical Engineering and Computer Science, University of California, Berkeley. This paper was recommended by Associate Editor M. Ogorzalek.

The author is with the Department of Electrical Engineering, Technical University of Eindhoven, 5600MB Eindhoven, The Netherlands.

Publisher Item Identifier S 1057-7122(96)01356-6.

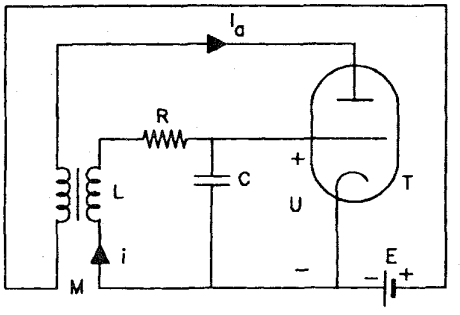

Fig. 2. Grid oscillator.

the tank circuit. Define U as the grid voltage, i as the current through the tank circuit and I_a as the plate or anode current. Then, under the assumption that the grid current $I_g = 0$, we can write

$$L\frac{di}{dt} + \frac{1}{C}\int i\,dt + R\cdot i = M\frac{dI_a}{dt} \tag{1}$$

with the term on the right site defining the voltage induced by the coupling coil with mutual inductance M. Further we have the relations of the tube,

$$I_a = SU, \quad U = \frac{1}{C}\int i\,dt \tag{2}$$

where S represents the transconductance of the tube T.

Equations (1) and (2) can be rewritten into

$$LC\frac{d^2U}{dt^2} + RC\frac{dU}{dt} + U = MS\frac{dU}{dt} \tag{3}$$

or

$$\frac{d^2U}{dt^2} + (2\alpha - \omega_o^2 MS)\frac{dU}{dt} + \omega_o^2 U = 0 \tag{4}$$

with $\alpha = R/2L$ and $\omega_o = 1/\sqrt{LC}$ defining the free oscillation frequency.

The factor α determines the rate of damping of the oscillation. When the term $2\alpha - \omega_o^2 MS$ becomes equal to zero we do not have damping. However, the oscillations will increase in amplitude when the term is negative. This can also be seen when we rewrite (3) into

$$L\frac{d^2U}{dt^2} + \left(R - \frac{MS}{C}\right)\frac{dU}{dt} + \frac{1}{C}U = 0. \tag{5}$$

Obviously, the feedback system inserts a negative resistance in the resonant circuit (defined by R, L, and C)

$$R' = -\frac{MS}{C}. \tag{6}$$

From this point of view the self excitation conditions consist of having the net resistance become negative,

$$R + R' = R - \frac{MS}{C} \le 0. \tag{7}$$

Normally, the relation between I_a and U is nonlinear and can be given as

$$I_a = a_o + a_1 U + a_3 U^3 + O(U) \tag{8}$$

from which it follows that

$$S = \left.\frac{dI_a}{dU}\right|_{\text{plate voltage constant}} = a_1 + 3a_3U^2. \tag{9}$$

Suppose that our circuit of Fig. 2 receives an incoming signal $A\cos(\omega t)$. The detection of this signal is normally achieved by an inductive coupling to L. Relation (4) changes under this influence into

$$\frac{d^2U}{dt^2} + \beta\frac{dU}{dt} + \omega_o^2 U = \omega_o^2 A\cos(\omega t) \tag{10}$$

with $\beta = 2\alpha - \omega_o^2 MS$.

Using (9) we can reformulate (10) into

$$\frac{d^2U}{dt^2} + (\beta_o + \gamma U^2)\frac{dU}{dt} + \omega_o^2 U = \omega_o^2 A\cos(\omega t) \tag{11}$$
$$\beta_o = 2\alpha - \omega_o^2 M a_1, \quad \gamma = -3\omega_o^2 M a_3.$$

Solving (11), we are searching for solutions of the form

$$B\sin(\omega t + \varphi) \tag{12}$$

for which the first derivative is given by

$$\frac{dU}{dt} = \sin(\omega t + \varphi)\frac{dB}{dt} + B\left(\omega + \frac{d\varphi}{dt}\right)\cos(\omega t + \varphi). \tag{13}$$

We are principally interested in the steady state, giving $dB/dt = d\varphi/dt = 0$ and hence we can rewrite (13) into

$$\frac{dU}{dt} = B\omega\cos(\omega t + \varphi). \tag{14}$$

Let us insert the solution (12) into (11) and discard terms containing the third harmonic in the substitution for $U^2(dU/dt)$. We also discard the term d^2B/dt^2 since B is a slowly varying function compared with $\sin(\omega t)$. For the left part this leads to

$$\begin{aligned} &-\omega^2 B\sin(\omega t + \varphi) + \beta_o B\omega\cos(\omega t + \varphi) \\ &\quad + \gamma B^2\left\{\frac{1}{2} - \frac{1}{2}\cos 2(\omega t + \varphi)\right\}B\omega\cos(\omega t + \varphi) \\ &\quad + \omega_o^2 B\sin(\omega t + \varphi) \\ &\approx (-\omega^2 B + \omega_o^2 B)\sin(\omega t + \varphi) + \left(\beta_o + \frac{\gamma}{4}B^2\right) \\ &\quad \cdot B\omega\cos(\omega t + \varphi) \end{aligned} \tag{15a}$$

and for the right part we will have

$$\omega_o^2 A\cos(\omega t) = \omega_o^2 A\{\cos\phi\cos(\omega t) + \sin\phi\sin(\omega t)\}. \tag{15b}$$

Now we separately equate the coefficients of $\sin(\omega t + \varphi)$ and $\cos(\omega t + \varphi)$ in the right and left halves, which will give us two equations

$$\begin{aligned} B(\omega_o^2 - \omega^2) &= \omega_o^2 A\sin\phi \\ \left(\beta_o + \frac{\gamma}{4}B^2\right)\omega B &= \omega_o^2 A\cos\phi. \end{aligned} \tag{16}$$

Squaring and adding (16) finally leads to

$$[(\omega_o^2 - \omega^2)^2 + \omega^2(\beta_o + \tfrac{1}{4}\gamma B^2)^2]B^2 = \omega_o^4 A^2. \tag{17}$$

When we further assume that the oscillator has the same frequency as the incoming signal, i.e., $\omega \approx \omega_o$ then we have

$$(\beta_o + \tfrac{1}{4}\gamma B^2)B = \omega_o A \tag{18}$$

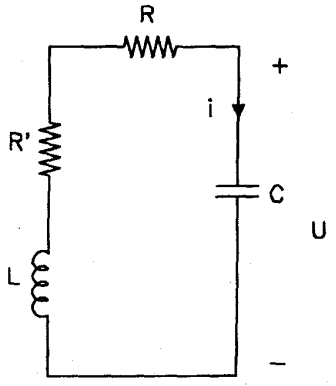

Fig. 3. Replacement circuit for the grid oscillator.

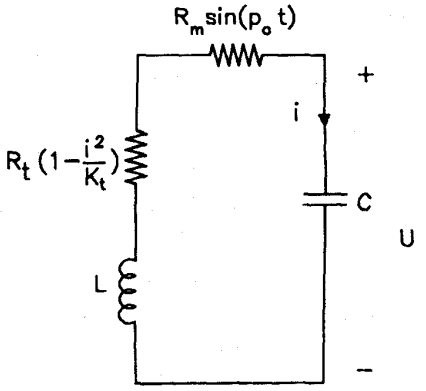

Fig. 4. Simplified model for the detector of Fig. 1.

Increasing the feedback factor will cause, at a certain moment, the circuit to oscillate. In this istuation the initial damping factor becomes

$$\beta_o = 2\alpha - \omega_o^2 M a_1 \approx 0 \tag{19}$$

which leads finally for the amplitude of U to be

$$B = \left(4\frac{\omega_o}{\gamma}A\right)^{1/3}. \tag{20}$$

Defining the sensitivity (or gain) as $g = dB/dA$, (20) will give us

$$g = \frac{1}{3}\left(4\frac{\omega_o}{\gamma}\right)^{1/3} \cdot A^{-2/3}. \tag{21}$$

From (21) it can be noted that for weak incoming signals, i.e., $A \ll 1$, the gain is extremely large. However, this is only the case when the circuit is tuned close to the incoming frequency. From (10) it is now obvious that the tube T acts to reduce the effective resistance of the tank circuit. This reduction in effective resistance can be considered as the introduction of a negative resistance by the tube. This means that one can treat the circuit of Fig. 2 as like that of Fig. 3.

As stated in the introduction, the circuit may not operate as oscillator, because in that state detection is not possible anymore. Armstrong solved this problem by making the effective negative resistance vary with time, at the quench frequency. When the total resistance is equal to or less than zero, the circuit oscillates. Detection of an incoming signal is possible just before the oscillation cycle starts. This circuit is called the super regenerative detector and is depicted in Fig. 1. The quench voltage induces a sinusoidal current in the plate circuit of the detector via L_q and C_q. This current alternates the total resistance of the tankcircuit via the inductive coupling M. The time constant determined by the LC product defines the free oscillation frequency as in Fig. 2 (and (4)).

III. Simplified Model

To understand more precisely the behavior of the quenching action of this type of detectors, a simplified model will be used. From the outline above, it became clear that the quench mechanism influences the total resistance of the tank circuit. Considering Fig. 3 we will make two assumptions to simplify this behavior. First, we substitute the equivalent variation of the effective resistance for the quench voltage $A\sin(2\pi pt)$. This effective resistance is composed of two terms:

- a periodic resistance $R_m \sin(p_o t)$ due to the quench action, with frequency $p = p_o/2\pi$ (Hz);
- a negative resistance due to the tube representing the nonlinear relation between the plate current I_a and the grid voltage U (see (8)). This resistance can be expressed as $R_t(1 - i^2/K_t)$ reflecting the quadratic coupling between the transconductance of the tube and the grid voltage. The component behaves as a current controlled resistor.

Second, we assume that the resistance of the remaining circuit can be neglected with respect to the other resistance's.

This finally leads to the equivalent circuit as shown in Fig. 4, for which the state equations in terms of the oscillation current in the tank circuit and the grid voltage are

$$\begin{aligned} L\frac{di}{dt} &= -U - iR_m \sin(2\pi pt) - iR_t\left(1 - \frac{i^2}{K_t}\right) \\ C\frac{dU}{dt} &= i \end{aligned} \tag{22}$$

or for which the differential equation (DE) can be expressed as,

$$\begin{aligned} \frac{d^2i}{dt^2} + \left[2\alpha\sin(p_o t) + \frac{R_t}{L}\left(1 - \frac{3i^2}{K_t}\right)\right]\frac{di}{dt} \\ + \left(\frac{1}{LC} + 2\alpha p_o \cos(p_o t)\right)i = 0 \end{aligned}$$

$$\alpha = \frac{R_m}{2L} \quad p_o = 2\pi p \tag{23}$$

This second-order DE is nonlinear and nonautonomous. Here the term LC defines the free oscillation frequency ω_o. This frequency is normally much higher than the quench frequency p_o. It is exactly the behavior of this equation we intend to investigate. However before doing so we will first show that (23) is consistent with the results previously obtained.

Suppose that the quench mechanism is removed ($p_o = 0$), then (23) becomes

$$\frac{d^2i}{dt^2} + \left[\frac{R_t}{L}\left(1 - \frac{3i^2}{K_t}\right)\right]\frac{di}{dt} + \left(\frac{1}{LC}\right)i = 0 \tag{24}$$

which has a form similar to (11) without excitation. If the nonlinearity in the circuit of Fig. 4 is omitted by assuming $R_t(1 - i^2/K_t) = 0$, the DE becomes the same as proposed by Ataka [8],

$$\frac{d^2i}{dt^2} + [2\alpha \sin(p_o t)]\frac{di}{dt} + \left(\frac{1}{LC} + 2\alpha p_o \cos(p_o t)\right) i = 0 \tag{25}$$

In this particular situation the DE can be transformed using the substitution

$$i = Iye^{((\alpha/p)\cos(p_o t))} \tag{26}$$

into

$$\frac{d^2y}{dt^2} + \left[\omega_o^2 - \frac{\alpha^2}{2} + p_o\alpha\cos(p_o t) + \frac{\alpha^2}{2}\cos(2p_o t)\right] y = 0. \tag{27}$$

This equation is a special form of Hill's equation, which can be transformed into a standard type of Mathieu's equation by a slight change of the independent variables [9], [10]. According to Ataka, the solution of DE (27) in this particular case can be given as

$$i = e^{((\alpha/po)\cos(p_o t))}\cos(\omega_o t + m\sin(p_o t)) \tag{28}$$

with $m = \alpha/2\omega_o$.

The following two figures are calculated from (28). In Fig. 5 the current i is plotted for a free frequency of $f_o = 5.0329$ Hz and a quench frequency of $p = 0.1592$ Hz. The quench amplitude R_m is set to 5 Ω. We see two sin "bursts" in the regions [1–4] (s) and [7–10] (s). Often the Lissajous figure is plotted, relating the current and the quench voltage with time t as a parameter. We will use $r(t) = R_m \sin(2\pi pt)$ as the plotting parameter. For the same situation the result is given in Fig. 6. In this figure we can define several events having as sequence: $S \rightarrow P \rightarrow E \rightarrow Q \rightarrow S$. The oscillation starts in point S at the moment for which the total resistance becomes negative and for which $r(t) \approx -4.2$ Ω. The amplitude of the current follows an exponential law (see also (28)) and increases rapidly in the direction towards $P(r(t) = -5\,\Omega)$. Then the amplitude decreases untill point E is reached for which the amplitude of the current becomes zero (in this situation $r(t) \approx 0$ Ω). From E to Q ($r(t) = 5$ Ω) and from Q to S there is no wave-oscillation in the receiver.

Although we (and Ataka) used a simplified model, the results fit well with the reported experiments done by Armstrong [1]. Researches like Armstrong expected that the noise of the circuit caused the start up of the free oscillation in point S of Fig. 6. Hence the start-up of the oscillations was irregular. This irregularity was noticed during measurements when plotting the Lissajous figure on the oscilloscope. The start-ups did not exactly take place in point S, which would give exactly one single point, but in a small region around this point. Hence, at the oscilloscope one noticed many spots around this point S, reported as "heavy spots" [1], [8], [13]. Also Ataka [8] reported this phenomenon, but was not able to reproduce this effect with his DE (28). In Fig. 6, there are indeed no irregularities. We shall demonstrate that including the nonlinearity imposed by the tube T, these irregularities will appear.

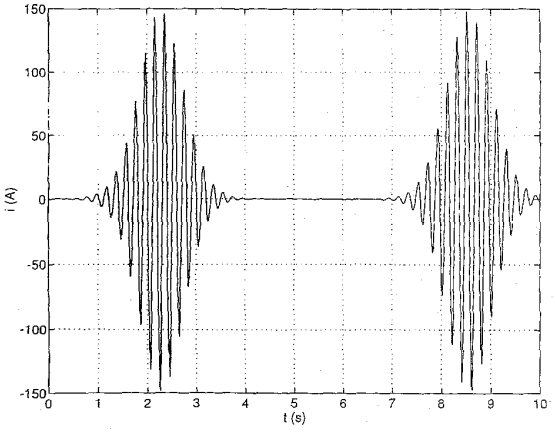

Fig. 5. Oscillatior current i for $p = 0.1592$ Hz. The plot is calculated from (28).

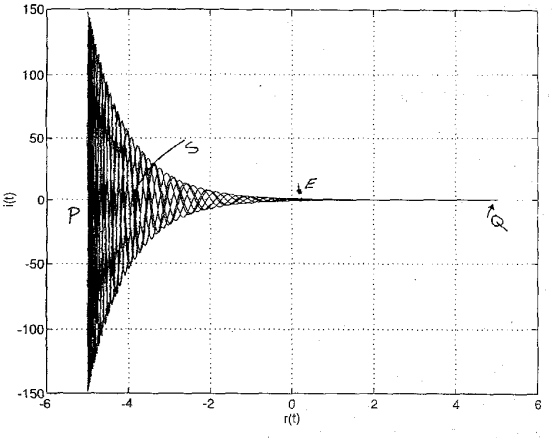

Fig. 6. Lissajous figure showing the relation between the oscillator current and the quench voltage for $p = 0.1592$ Hz. The plot is calculated from (28).

IV. Chaotic Behavior in the Detector

For the remaining part of this section, we will focus ourselves on the DE of (23), conform Fig. 4, assuming the following parameters values, unless otherwise stated

$$\begin{aligned} R_m &= 100\ \Omega \\ R_t &= -1\ \Omega \\ K_t &= 50\ \mathrm{A}^{-2} \\ L &= 1\ \mathrm{H} \\ C &= 0.001\ \mathrm{F} \end{aligned} \tag{29}$$

The free oscillation f_o is in this situation 5.0329 Hz, while the quench frequency p will be varied (see (23)). All simulations were performed using a fourth-order Runge–Kutta method where the stepsize was adapted to the problem under consideration. Although we used exisiting routines for the computation, all simulations are cross checked with the program INSITE, which was specially developed to analyse nonlinear dynamical

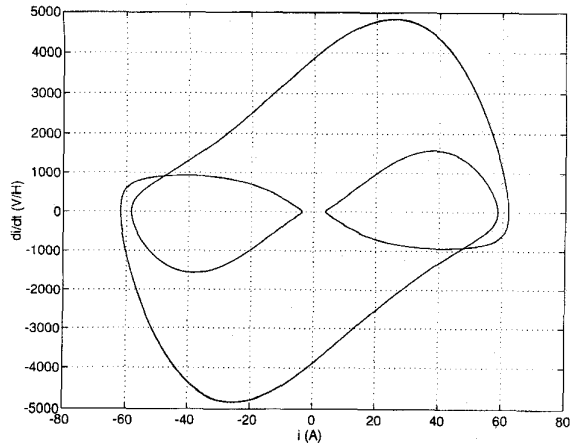

(a)

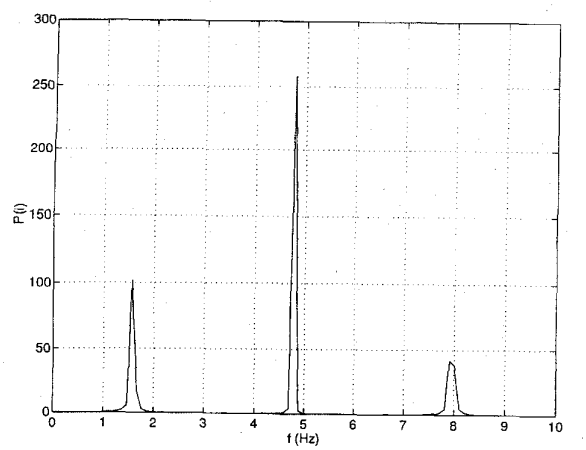

(b)

Fig. 7. Periodic behavior for $p = 3.1831$ Hz. The other parameters are equal to (29). Shown are the phase diagram (a) and the frequency spectrum (b).

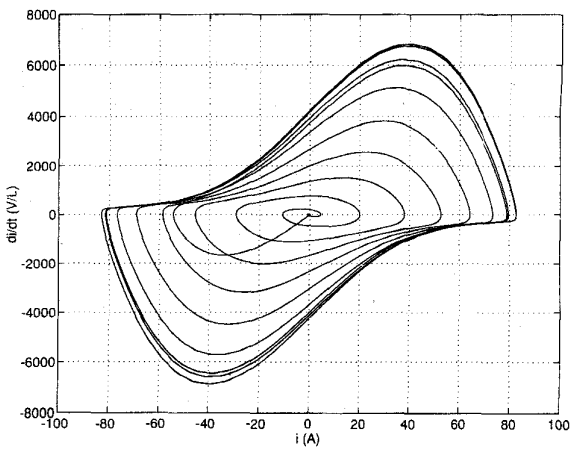

(a)

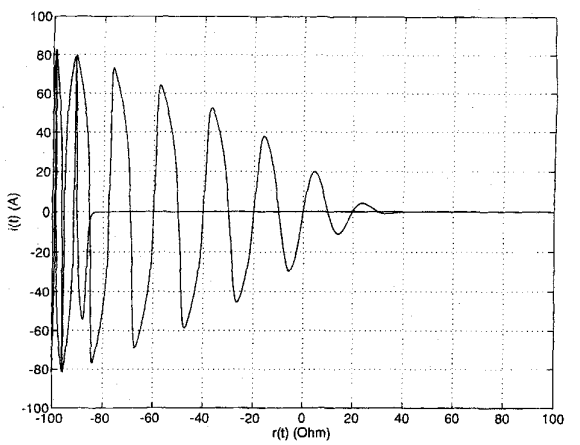

(b)

Fig. 8. Quasi-stationary behavior for $p = 0.1592$ Hz. The other parameters are equal to (29). Shown are the phase diagram (a) and the Lissajous figure (b).

systems [16]. For the spectrum analysis, an FFT of 1024 points was used.

The detector can operate in two modes, a "state of modulation" and a "state of quenching." In the state of modulation the ratio f_o/p is too small, the free oscillation frequency will be amplitude modulated by the quenching oscillation frequency. It is not possible to detect any incoming signal in this situation. This situation can be simulated using $p = 3.1831$ Hz. The phase diagram shows indeed a period-3 trajectory (Fig. 7(a)), for which the frequencies can be deduced from Fig. 7(b). We can observe that the amplitude of the free oscillation frequency is indeed modulated by the quenching oscillation.

By gradually decreasing the frequency p to 0.1592 Hz, one reaches the so-called "state of quenching". This situation is depicted in Fig. 8(a), where a quasi-stationary behavior can be observed. Each time, the oscillation starts up under the same conditions at period p. There is no irregular behavior, which becomes also clear from Fig. 8(b). In this figure the points $E(r(t) = 40\,\Omega)$ and $S(r(t) = -85\,\Omega)$, as defined in Fig. 6, are clearly visible.

Consider finally the situation in which $p = 0.0318$ Hz. The ratio f_o/p becomes large and this ratio, or a larger ratio, is used in real practice. For this situation Fig. 9(a) shows the phase diagram and Fig. 9(b) the frequency spectrum, the latter having a continuous broad-band nature. Such a spectrum is typical for systems showing chaotic behavior. To show that in this situation the behavior of the current is indeed irregular, we will use the Poincaré map (see for instance [11], [12]).

For that purpose, the state equations in the Euclidian space of (22) will be transformed into third order autonomous state equations in the cylindrical space

$$\begin{aligned}
\frac{di}{dt} &= U \\
\frac{dU}{dt} &= -\left[2\alpha \sin\left(p_o \frac{\theta T}{2\pi}\right) + R_t\left(1 - \frac{3i^2}{K_t}\right)\right] U \\
&\quad - \left[\frac{1}{LC} + 2\alpha p_o \cos\left(p_o \frac{\theta T}{2\pi}\right)\right] i \\
\frac{d\theta}{dt} &= \frac{2\pi}{T}
\end{aligned} \tag{30}$$

(see for instance [12]).

The Poincaré map will be computed for several locations on the line QP in Fig. 6. For sake of clearness, we stretch

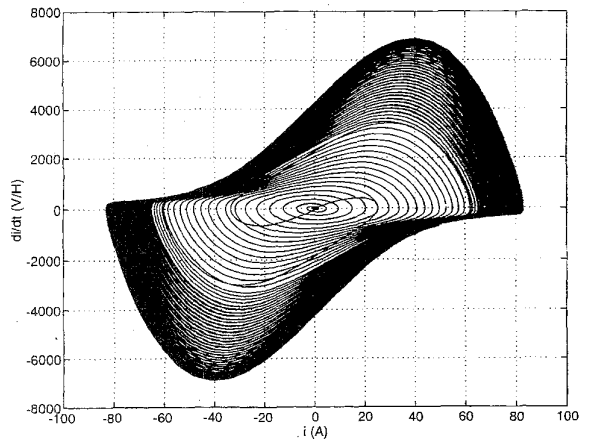

(a)

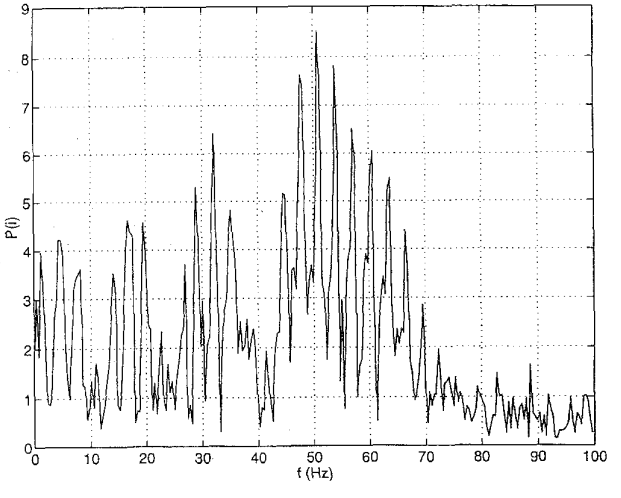

(b)

Fig. 9. Irregular behavior for $p = 0.0318$ Hz. The other parameters are equal to (29). Shown are (a) the phase diagram and (b) the frequency spectrum.

Fig. 6 and draw the Poincaré planes in it as can be seen in Fig. 10. Consider plane Σ_1, for which two closed curves are to be expected, as there are in this state two frequencies of main importance. Fig. 11(a) shows two closed orbits, the outer trajectory is due to the quenching, the inner represents the dying free oscillation. If the plane is shifted towards Q the inner trajectory will completely disappear, i.e., the oscillation dies out. In the region of point S the irregularities, as reported in the literature, were assumed to represent the characteristic noise of the system. Fig. 11(b) shows the Poincaré map as we use plane Σ_2 for which $r(t) = -58.79\,\Omega$. The closed trajectory is due to the quench action of the oscillator, but there are also some irregular spots. Fig. 11(c) is the map for Σ_3 in the neighborhood of S on the line $SP\,(r(t) = -60.0\,\Omega)$. Fig. 11(d) shows the map for which the plane is more located in the neighborhood of $P\,(r(t) = -68.8\,\Omega)$. It becomes clear that the irregular behavior disappears and that the contour of a limit set becomes visible. The limit set represents the self sustained oscillation of the system at that moment.

From the computer simulations above, we can see that the behavior of the oscillator current is irregular during the

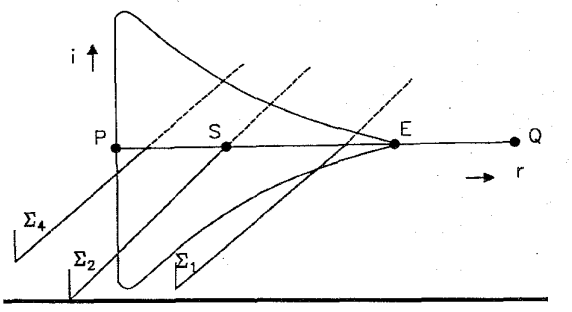

Fig. 10. Different locations of the Poincaré plane: Σ_1 at $r(t) = 6\,\Omega$, Σ_2 at $r(t) = -58.79\,\Omega$, and Σ_4 at $r(t) = -68.8\,\Omega$. The plane Σ_3 at $r(t) = -60.0\,\Omega$ is left out for sake of clearness.

first few moments when the total resistance of the circuit is negative. After this small period, the resistance is such that the circuit behaves like an oscillator. The oscillation dies out when the total resistance becomes positive and the cycle starts again. The quench mechanism controls the total resistance and in that way also the chaotically operating mode.

Lyapunov exponents describe the (averaged) expansion and contraction rates of small perturbations in different directions of the state space on a logarithmic scale. For a 2-D system a strange attractor must have one positive and one negative Lyapunov exponent, λ_+ and λ_-, respectively, while the sum must be negative. The positive exponent is related to the property of high sensitivity on initial conditions and the system may be termed chaotic. The Lyapunov dimension is then defined as

$$D_L = 1 + \frac{\lambda_+}{|\lambda_-|}. \tag{31}$$

Lyapunov exponents are related to the steady-state behavior of a system. Although the quenching mechanism makes it difficult to define for the oscillator what the steady-state situation is, the complete system, including the quench action, reaches a steady state.

The Lyapunov exponents for the situation $p = 0.0318$ Hz are $\lambda_+ = 0.42094$ and $\lambda_- = -37.459$, leading to a Lyapunov dimension of $D_L = 1.01124$. The circuit exhibits irregular behavior. For the situation with $p = 3.1831$ Hz the exponents are $\lambda_+ = -2.9231$ and $\lambda_- = -57.0177$ and the circuit exhibits periodical behavior.

From the figures it turns out that the start-up conditions are indeed irregular for this type of oscillator. It is exactly this chaotic behavior that in the literature is described as "heavy spots" and have been heard and seen during experiments as characteristic noise. It means that this type of detectors has an operating "characteristic" starting from a quiescent mode, followed by chaos and finally becoming an oscillator, for which the oscillation eventually dies out. After a small period the cycle starts again.

V. Amplification via Chaos

Amplification in such detector systems is defined as the difference Δi in the amplitude of the current in the case of receiving an unmodulated input signal and the amplitude of the

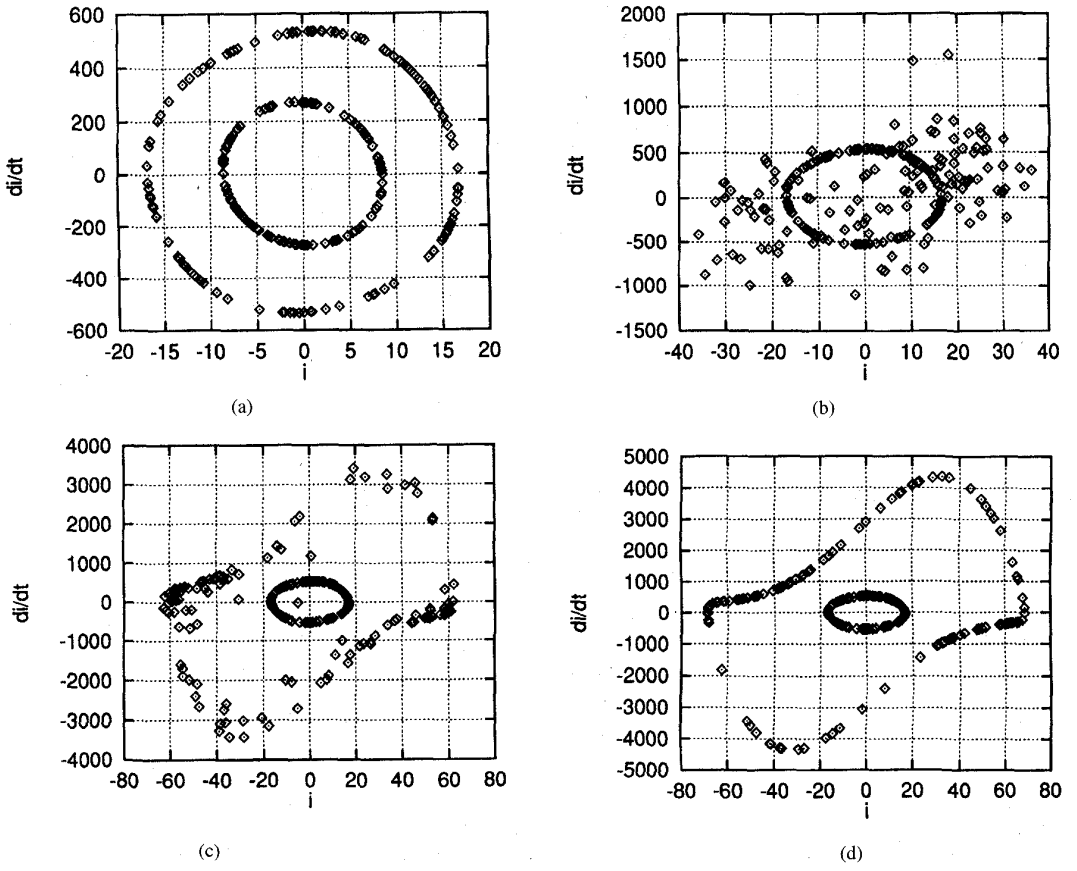

Fig. 11. Poincaré maps for $p = 0.0318$ Hz. The other parameters are equal to (29). The maps are generated for differnt values of $r(t)$: (a) $r(t) = 6\,\Omega$, (b) $r(t) = -58.79\,\Omega$, (c) $r(t) = -60\,\Omega$ and (d) $r(t) = -68.8\,\Omega$.

TABLE I
AMPLIFICATION FOR SETTINGS OF (29)

Quench frequency p (Hz)	Amplification Δi (A)
0.7958	0.1
0.3183	0.5
0.1592	57
0.0318	63
0.0159	53
0.0080	70

current without any incoming signal. This difference is then squared by the tube characteristic and can be detected on the plate voltage U. Ataka as well as Frink [13] noticed that the amplification of the detector depends on the quench frequency. There was only a small range of frequencies possible in which they obtain amplification. For several quench frequencies the amplification is computed (Table I). Because the detection is maximal when the oscillation frequency is tuned to the incoming signal frequency (see (17) and (21)), a sine wave with an amplitude of 1 V and a frequency of 5.0329 Hz (thus exactly the free-oscillation frequency of the detector) is used as input signal.

In the state of modulation, the amplification is low. The gain rapidly increases in the state of quenching. For the region in which chaotic behavior is observed ($p \leq 0.0318$ Hz) the amplification is higher than in the situation where this behavior is not observed. An exception is the quenching frequency $p = 0.0159$ Hz, where probably the chaotic energy level is locally decreased. We might say that the best operation mode for the detector is the state of quenching in which the start up behavior is chaotic. This is in agreement with the experimental results of Ataka and Frink. Both stated that the best operating point of the super regenerative could be identified with the situation where the "heavy spots" in the Lissajous figure would occur. In that situation the ratio f_o/p is large. In the detector, the amplification seems to be closely related to chaos. Amplification via chaos is already observed in the circuit proposed by Chua [14], [15]. Also in Chua's circuit the amplification achieved the highest value when the circuit operates in the chaotic regime. For this circuit it was already mentioned that amplification via chaos leads to the possibility of highly sensitivity detectors. In the super regenerative detector the high sensitivity is just caused by the extraordinary amplification.

VI. CONCLUSION

It turns out that the super regenerative detector, as developed by Armstrong, achieves its high amplification in the operating mode where chaotic behavior is observed. It is exactly this

region where irregularities were observed in past measurements. These irregularities were believed to be related to the characteristic noise of the circuit. However, the nonlinearity of the tube influences the behavior of the oscillation current. This results in an irregular behavior of the current just before the circuit operates as oscillator. The detector has an operating sequence from quiescent mode followed by chaos mode and finally an oscillation mode. The oscillation will eventually die out and the operating mode becomes the quiescent mode. When the circuit is tuned such that the behavior of the current is irregular, the amplification of incoming signals is maximal.

ACKNOWLEDGMENT

The author is grateful to Prof. L. Chua of the University of California, Berkeley for valuable discussions on the subject and to Prof. W van Bokhoven of the Eindhoven University of Technology for his suggestions in this research. Also some helpful comments from the reviewers were appreciated.

REFERENCES

[1] E. H. Armstrong, "Some recent developments of regenerative circuits," *Proc. Inst. Radio Eng.*, vol. 10, no. 8, pp. 244–260, 1922.
[2] J. L. Eaves and E. K. Reedy, *Principles of modern Radar*. New York: Van Nostrand Reinhold, 1987.
[3] B. van der Pol and J. Van der Mark, "Frequency demultiplication," *Nature*, vol. 120, pp. 363–364, 1927.
[4] M. P. Kennedy and L. O. Chua, "Van der Pol and chaos," *IEEE Trans. Circuits Syst.*, vol. CAS-33, pp. 974–980, 1986.
[5] Y. Ueda and N. Akamatsu, "Chaotically transitional phenomena in the forced negative-resistance oscillator," *IEEE Trans. Circuits Syst.*, vol. CAS-28, pp. 217–223, 1981.
[6] G. Mamola and M. Sannino, "Analysis of negative-resistance oscillators with piecewise nonlinearity," *Circuit Theory Appl.*, vol. 5, pp. 287–297, 1977.
[7] H. Tarukawa *et al.*, "Chaos generated in the forced Rayleigh oscillator," in *Proc. ECCTD*, Davos, Switz., 1993, pp. 631–636.
[8] H. Ataka, "On superregeneration of an ultra-short-wave receiver," *Proc. Inst. Radio Eng.*, vol. 23, pp.841–885, 1935.
[9] W. Magnus, S. Winkler, *Hill's Equation*. New York: Intersci., 1966.
[10] N. W. McLachlan, *Theory and applications of Mathieu functions*. New York: Clarendon, 1951.
[11] T. S. Parker and L. O. Chua, "Chaos: A tutorial for engineers," *Proc. IEEE*, vol. 75, pp. 982–1007, Aug. 1987.
[12] ——, *Practical Numerical Algorithms for Chaotic Systems* New York: Springer-Verlag, 1989.
[13] F. W. Frinck, "The basic principles of super-regenerative reception," *Proc. Inst. Radio Eng.*, vol. 26, pp.76–106, 1938.
[14] L. O. Chua and G. Lin, "Canonical realization of Chua's circuit family," *IEEE Trans. Circuits Syst.*, vol. 37, pp. 885–902, July 1990.
[15] K. S. Halle, L. O. Chua, V. S. Anishchenko, and M. A. Safonova, "Signal amplification via chaos: Experimental evidence," in *Chua's circuit, A paradigm for CHAOS*, R. N. Madan, Ed. Singapore: World Scientific, 1993.
[16] T. S. Parker and L. O. Chua, "INSITE—A software toolkit for the analysis of nonlinear dynamical systems," *Proc. IEEE*, vol. 75, pp. 1081–1089, 1987.

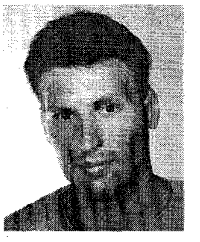

Domine M. W. Leenaerts (M'94) received the Ir. and the Ph.D. degrees in electrical engineering from the Eindhoven University of Technology in 1987 and 1992, respectively.

Since 1992 he has been with the same University as an Assistant Professor of the microelectronic circuit design group. In 1995, he was a Visiting Scholar with the Department of Electrical Engineering and Computer Science of the University of California, Berkeley. His research interests includes nonlinear dynamic system theory, chaotic behavior in circuits and analog design automation. He has published several papers in scientific and technical journals and conference proceedings.